Biochemical and Biophysical Research Communications 529 (2020) 548–553

Contents lists available at ScienceDirect

Biochemical and Biophysical Research Communications

journal homepage: www.elsevier.com/locate/ybbrc

Structure of a robust bacterial protein cage and its application as a versatile biocatalytic platform through enzyme encapsulation

Nikola Lončar [a], Henriette J. Rozeboom [b], Linda E. Franken [c, 1], Marc C.A. Stuart [c], Marco W. Fraaije [b, *]

[a] GECCO Biotech, Nijenborgh 4, 9747AG, Groningen, the Netherlands
[b] Molecular Enzymology Group, University of Groningen, Nijenborgh 4, 9747AG, Groningen, the Netherlands
[c] Department of Electron Microscopy, University of Groningen, Nijenborgh 7, 9747, AG, Groningen, the Netherlands

ARTICLE INFO

Article history:
Received 5 June 2020
Accepted 12 June 2020
Available online 15 July 2020

Keywords:
Encapsulin
Crystal structure
Enzyme stability
Biocatalysis
Cofactor

ABSTRACT

Using a newly discovered encapsulin from *Mycolicibacterium hassiacum*, several biocatalysts were packaged in this robust protein cage. The encapsulin was found to be easy to produce as recombinant protein. Elucidation of its crystal structure revealed that it is a spherical protein cage of 60 protomers (diameter of 23 nm) with narrow pores. By developing an effective coexpression and isolation procedure, the effect of packaging a variety of biocatalysts could be evaluated. It was shown that encapsulation results in a significantly higher stability of the biocatalysts. Most of the targeted cofactor-containing biocatalysts remained active in the encapsulin. Due to the restricted diameters of the encapsulin pores (5–9 Å), the protein cage protects the encapsulated enzymes from bulky compounds. The work shows that encapsulins may be valuable tools to tune the properties of biocatalysts such as stability and substrate specificity.

1. Introduction

Compartmentalization of the cell's interior to create distinct organelles is a defining hallmark of eukaryotes. This provides these cells with a way to separate and optimize metabolic processes. Although typical membrane-encompassed organelles are lacking, bacteria have found other ways to compartmentalize enzymes by using proteinaceous structures. While the reason for bringing together a selected set of enzymes within a protein shell is not always clear, bacterial microcompartments are conserved and widespread in the bacterial kingdom [1,2]. This strongly suggests that they are essential for proper functioning of the encapsulated enzymes. This type of subcellular co-localization may be to facilitate substrate transfer between connected reactions and to shield the separated metabolism from interference by other cellular components. Moreover, encapsulation of enzymes within a protein cage can promote the reaction rate as a consequence of the high effective concentration of enzyme, which leads to rapid formation of the enzyme–substrate complex [3,4]. Experimental work done on the different bacterial protein-based compartments has revealed that the selective incorporation of target proteins depends on N- or C-terminal recognition peptides [5,6]. This is similar to protein targeting in eukaryotic organelles, such as the N- or C-terminal peroxisomal targeting sequences [7]. Bacterial microcompartments are normally larger (50–200 nm) and composed of several building proteins while encapsulins are much smaller and composed of only one protein.

Only about a decade ago a newly recognized class of bacterial protein-based nanocompartments was described [8]. These so-called encapsulins are formed by self-assembly of 60 or 180 identical encapsulin protomers to form cages with a diameter of roughly 24 or 32 nm, which are divided into four families [2]. In Nature, these bacterial protein cages typically contain one or a few different proteins, often enzymes. The encapsulated proteins are targeted to the interior of encapsulins by virtue of a N- or C-terminal targeting peptide. The rationale for the translocation of specific proteins into encapsulins is still enigmatic. In most cases, encapsulins contain a ferritin-like protein or a dye-decolorizing peroxidase (DyP), while in some other cases other metal-containing proteins have been identified [9]. A general feature of the cargo proteins seems to be an

* Corresponding author.
E-mail address: m.w.fraaije@rug.nl (M.W. Fraaije).
[1] Present Address: Department of Structural Cell Biology of Viruses, Heinrich-Pette-Institut, Leibniz-Institut für Experimentelle Virologie - Centre for Structural Systems Biology, Notkestraße 85, 22607, Hamburg, Germany.

https://doi.org/10.1016/j.bbrc.2020.06.059

involvement in redox processes, and therefore it has been hypothesized that encapsulins play a role in detoxification processes.

Several viral nanoparticles and bacterial microcompartments have been produced as recombinant proteins and have been studied with various cargo proteins in the context of fundamental science, nanotechnology or as a tool in cell biology [9–17]. Examples of benefits of encapsulation are the encapsulation of a hydrogenase and multiple enzymes in bacteriophage capsids which improved the stability of the respective enzymes [18,19]. It has also been shown that foreign proteins can be targeted to encapsulins [20]. This served as starting point to explore the value of these protein cages for biocatalysis. In this work, we describe the structural features of an encapsulin originating from the mesothermophile *Mycolicibacterium hassiacum* (EncMh) and its use as protein cage for several biocatalysts. Except for establishing a highly effective production procedure for this robust encapsulin, we elucidated its structure by cryo-electron microscopy and X-ray crystallography. Furthermore, we demonstrate that various enzymes can be packaged in EncMh and be used as highly stable encapsulated biocatalysts.

2. Materials and methods

Details on the materials and methods used can be found in the Supporting Information.

2.1. Strains, plasmids and co-expression vectors

Escherichia coli NEB10β was used for routine cloning and expression of EncMh. The gene encoding EncMh (YP_289707.1) was synthesized as codon optimized for *E. coli* by GeneScript. Expression of EncMh was performed using a pBAD vector. Genes of the cargo proteins were cloned into the pENC vector in order to be compatible with the pBAD vector. Cargo protein was expressed with a N-terminal 6xHis-tag and the C-terminal targeting tag. For co-expression, pBAD-EncMh and pENC-cargo were co-transformed into *E. coli* BL21-AI (ThermoFisher).

2.2. Expression and purification of encapsulin and cargo enzymes

Expression of encapsulin and cargo enzyme was initiated by adding 1 mM IPTG and 0.2% arabinose. Cultures were then incubated for 16–20 h at 30 °C and then harvested using centrifugation and sonicated on ice. After centrifugation, the cleared cell-free extract was loaded on a Ni-Sepharose column to remove the excess of cargo-enzyme. For precipitation of EncMh, flow-through fractions were mixed on ice with equal volumes of 10% PEG-8000 solution, 50 mM TrisHCl pH 7.5, 2 M NaCl. If needed, polishing was done using a Superdex 200 column with 50 mM TrisHCl at pH 7.5 and 150 mM NaCl. Encapsulin and encapsulin loaded with cargo enzyme eluted in the void volume.

2.3. Proteolytic resistance of encapsulin

Purified encapsulin (10 mg/mL) was incubated for 16 h with bovine trypsin and Proteinase K to study resistance to proteolytic degradation. Trypsin from bovine pancreas (1 mg/mL) was in 50 mM acetate buffer, while Proteinase K from *T. album* (1 mg/mL) was in 50 mM TrisHCl pH 8.0 with 10 mM $CaCl_2$. Reactions contained 50 μL of 10 mg/mL EncMh, 400 μL TrisHCl pH 8, 10 mM $CaCl_2$, 2 mM DTT and 50 μL of protease solution. Samples were incubated at 37 °C for 16 h and were then analyzed by SDS PAGE.

2.4. Cryo-transmission electron microscopy and X-ray crystallography

Details on structural analyses of EncMh can be found in the Supporting Information. Figures were prepared with PyMOL [21] and ESPript [22]. Atomic coordinates and experimental structure factor amplitudes for EncMh have been deposited in the RCSB Protein Data Bank and are accessible under entry code 6I9G.

3. Results and discussion

3.1. Overall structure of the Mycolicibacterium hassiacum encapsulin

M. hassiacum is an actinobacterium which tolerates temperatures up to 65 °C [23]. By analyzing its genome for encapsulin homologs we identified a small operon consisting of two genes encoding a putative encapsulin (EncMh, WP_005630281.1) and a putative DyP-type peroxidase (EKF22245.1). The putative encapsulin has a predicted molecular mass of 29 kDa and shares 34% sequence identity with the encapsulin from *Thermotoga maritima* [8]. The putative DyP carries a C-terminal sequence that resembles the targeting sequence used for incorporation into encapsulins. Based on these observations we decided to clone the gene encoding for EncMh for expression in *E. coli*. Upon screening expression conditions, we achieved a remarkably high expression level. SDS-PAGE analysis revealed that most of the intracellular protein was EncMh. While EncMh could be purified to homogeneity by column chromatography (Fig. S1), we also developed a simple purification protocol that merely depends on the selective precipitation of EncMh by 5% PEG8000. Both purification procedures yield an impressive amount of 1 g purified EncMh from 1 L growth medium, making EncMh an interesting candidate for further studies. EncMh was found to be resistant to proteolytic degradation by bovine trypsin and proteinase K (Fig. S2), as reported for other encapsulins [20]. Additionally, EncMh displays a high thermostability as the oligomeric state was found to be stable up to 50 °C (Fig. S3). As expected for encapsulins, gelpermeation already suggested that EncMh forms large oligomers. Cryo-electron microscopy analysis revealed that EncMh forms large spherical structures with a diameter of about 22 nm, which is in line with other reported data on encapsulins with a T = 1 symmetry [9]. By class averaging an icosahedral architecture became apparent (Fig. 1). For a more detailed structural analysis, we set out to crystallize EncMh. This

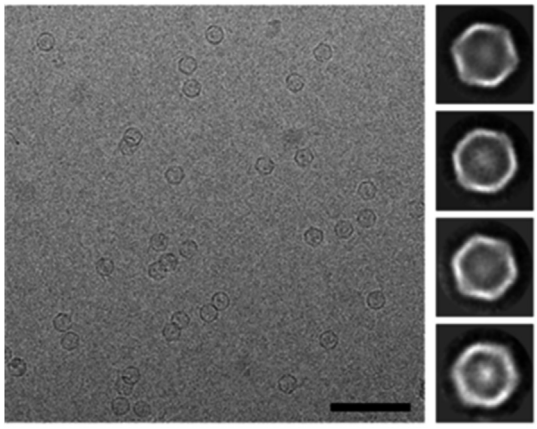

Fig. 1. (Left) A typical micrograph of EncMh (scale bar: 100 nm). (Right) Four representative class averages of particles: images are the average sum of 1299, 602, 559 and 218 particles (top to bottom).

resulted in well-diffracting crystals and allowed us to determine a high-resolution structure of EncMh. The 2.5 Å electron density map showed continuous density for all residues (1–265) in all fifteen chains (A-O) in the asymmetric unit and has an R/Rfree of 17.2/21.1%. Data collection and phasing details are summarized in Table S1. Five protein chains form a pentamer and the T = 1 icosahedral capsid is composed of 12 pentameric EncMh oligomers (Fig. 2). The unit cell contains two icosahedrons with a diameter of 23 nm and a thickness of the protein layer of 2.0–2.5 nm. These data are perfectly in line with the CryoEM data. A comparison of EncMh with other capsid proteins shows that it is most similar to the encapsulin from *T. maritima* (PDB 3DKT) [8]with a RMSD value of 1.8 Å on 251 Cα atoms. The EncMh monomer shows the HK97 fold, the principal fold of many capsids, and consists of a P-domain (peripheral domain), A-domain (axial domain) and E-loop (extension loop) (Fig. S4) [24]. Its N-terminus is located on the inside of the capsule while the C-terminus is on the outside. The P-domain (residues 1–43, 77–135 and 220–254) is composed of a three-stranded antiparallel β-sheet (β4-β11-β12) with on one side two small and two long α-helices (α1-α4). A small F-loop (44–46) is inserted after α2 and the E-loop (47–76) is inserted which consists of a kinked two-stranded β-sheet (β2-β3) and is involved in the two-fold interaction in EncMh (Fig. S4). Helix α4 contains a 9 residue excursion; Gly122-Gly130, called the G-loop [24]. The A-domain (residues 136–219 and 254–265) is composed of a mixed five-stranded β-sheet (β5-β6-β9-β10-β13), called β-hinge, that links the A- and P-domains of HK97-like proteins and is flanked by three α-helices (α5-α7) [24]. Interestingly, Cys134, the ultimate residue of α4, is involved in a disulfide bridge with Cys254, the ultimate residue of β12 from the P-domain. This disulfide is not observed in structures of known homologous encapsulins and may contribute to the stability of EncMh.

The tip of the A-domain is involved in the icosahedral five-fold axis (Fig. S5). At this axis an opening is present with a diameter of 8 Å diameter which is shaped by His187-Gly-Tyr189 together with Arg197. One of the bound sulfate ions occupies the entrance to the capsid at the five-fold axis while 5 sulfate ions are bound close to the entrance. The three-fold axis is located near the N-terminus where no clear pore can be identified. However, two additional pores are present at the interface of two monomers, one with a diameter of 9 Å and one with a diameter of 5 Å (Fig. S6). The pore diameters are similar to the pores of carboxysomes and metabolosomes that contain pores with a diameter of 4–10 Å [25].

3.2. Development of EncMh as protein encapsulation platform

Having a robust encapsulin at hand which can be easily expressed and isolated, we explored EncMh as packaging protein for biocatalysts. The generated encapsulated biocatalysts were tested for beneficial effects exerted by being packaged in EncMh. We have explored the encapsulation of biocatalysts from different enzyme classes (catalases, monooxygenases, oxidases, and peroxidases), containing different types of cofactors (heme, flavin and copper), and of different sizes (up to 270 kDa) (Figs. S7–S11). For targeting the enzymes to the interior of EncMh, a C-terminal 30 residues peptide (PPPLPDSEPDREIPADDGSLGIGSLKGTRS) was added to each enzyme. This targeting peptide is used by the native DyP of *M. hassiacum*. Co-expression of EncMh and each target enzyme was accomplished by using a two-plasmid system (for details on vector design see SI). Co-precipitation of EncMh with cargo protein during PEG precipitation and co-elution upon gel-permeation was taken as proof of successful loading of EncMh. CryoEM was used to verify that cargo protein had not aggregated on the outside of EncMh (Fig. S12).

As initial test we examined whether a small heme-containing protein, bacterial hemoglobin VsHb (WP_019959060.1), could be packaged in EncMh by coexpressing both proteins. VsHb was cloned with and without C-terminal targeting peptide resulting in proteins of 21 kDa and 18 kDa, respectively. These two proteins were individually coexpressed with EncMh. VsHb with the encapsulation tag could be clearly observed in the isolated red-colored EncMh, while the VsHb without encapsulation tag did not coprecipitate with EncMh but ended up in the soluble fraction. This demonstrates that the employed C-terminal tag is efficient in loading EncMh with foreign cargo proteins (Fig. S4). Next, we decided to test loading of EncMh with various enzymes.

3.3. Encapsulation of a peroxidase and laccase by EncMh

First, a bacterial peroxidase, DyP from *Saccharomonospora viridis* DSM43017 (SviDyP), was successfully packaged in EncMh. This peroxidase was recently shown to be active on various dyes and showed potential in modifying lignin-containing biomass [26]. Purification included, except for PEG precipitation, an affinity chromatography step to remove any traces of non-encapsulated SviDyP. Both EncMH and SviDyP were well expressed as evidenced by SDS-PAGE analysis (Fig. S7). The obtained protein

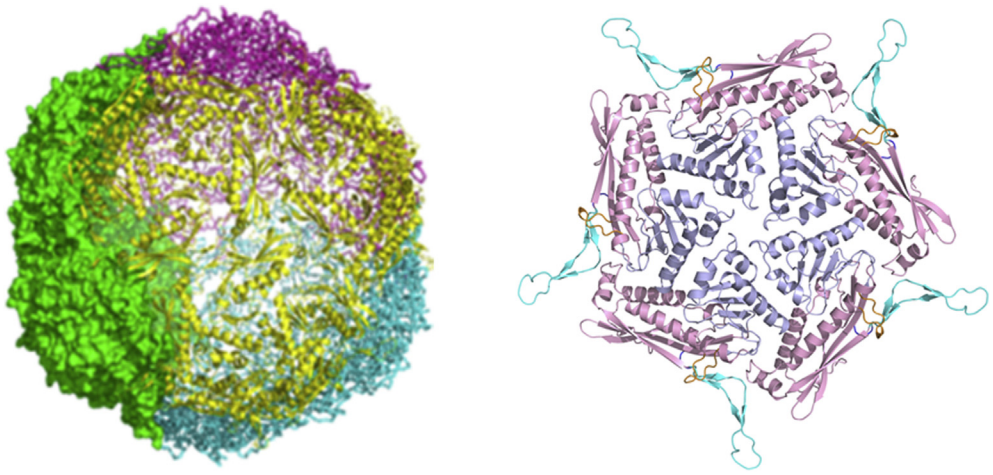

Fig. 2. Crystal structure of EncMh (PDB:6I9G). Left: the 60-meric EncMh with three pentameric units in yellow. Right: a pentamer with protomers in different colors. (For interpretation of the references to color in this figure legend, the reader is referred to the Web version of this article.)

sample contained only the two overexpressed proteins and displayed a clear red color due to the presence of the heme cofactor in SviDyP. Gel permeation confirmed that the peroxidase had been incorporated in the encapsulin. The packaged peroxidase was found to be active on ABTS, a commonly used peroxidase substrate [27]. Using ABTS as test substrate, we examined the effect of encapsulation on the kinetic parameters of SviDyP (Fig. 3). Non-encapsulated enzyme displayed a k_{cat} of 24.5 ± 0.9 s^{-1} and a K_m of 0.15 ± 0.02 mM while encapsulated SviDyP displayed a slightly lower k_{cat} (17.9 ± 1.9 s^{-1}) and higher K_m (0.55 ± 0.1 mM). Whether the packaging in EncMh has a stabilizing effect on the peroxidase was tested by incubating the encapsulated enzyme and the free enzyme at 40 °C and monitoring peroxidase activity in time. This revealed that the packaging in EncMh has a strongly stabilizing effect (Fig. S13). While the unpackaged peroxidase lost its activity within 30 min, the packaged peroxidase showed even an increase in activity in the first few hours and only after 25 h the activity decreased significantly (Fig. S13). The increase in activity upon incubation at higher temperature of enzymes from (semi)thermophiles has been observed before [28,29] and may suggest that an optimal catalytically competent conformation is attained at a higher temperature. The stabilizing effect of encapsulation may also be due to a molecular crowding effect: the intense protein-protein interactions in the capsule prevents irreversible unfolding and aggregation of the cargo protein.

We also coexpressed a bacterial copper-containing oxidase, a laccase, with EncMh. This resulted in an encapsulated laccase as evidenced by the green appearance of the isolated encapsulin preparation. Activity of the laccase in EncMh was verified using syringaldazine (MW 360 g/mol). As the bacterial laccase is already highly thermostable [30], we were not able to assess the effect of encapsulation on thermostability.

3.4. Loading of EncMh with a large catalase

To challenge the capacity of EncMh, we also coexpressed a tetrameric heme-containing catalase of 270 kDa from *Thermobifida fusca* (TfuCat) [31]. Encapsulation of TfuCat was successful as indicated by the isolation of intensely brown-colored encapsulin. The encapsulation of TfuCat shows that EncMh can accommodate cargo proteins ranging from 17 kDa (VsHb) to relatively large cargo proteins such as catalase. The packaged catalase retained activity on hydrogen peroxide and was also able to oxidize catechol, as was reported for the isolated enzyme [31]. Encapsulated TfuCat showed similar behavior as SviDyP. Upon encapsulation, TfuCat displayed a slightly lower catalytic efficiency (k_{cat}/Km) when compared with the non-encapsulated catalase (0.7 vs. 1.6 × 10^6 $s^{-1}M^{-1}$).

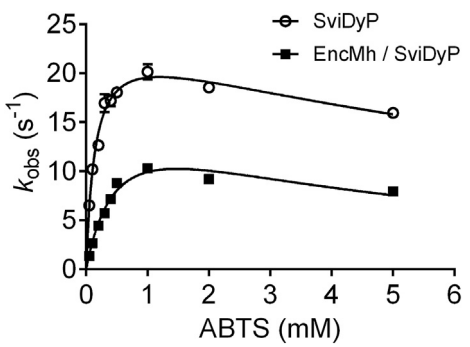

Fig. 3. The effect of encapsulation on activity of SviDyP.

3.5. Encapsulation of flavoenzymes by EncMh

The loading of flavoenzymes was tested as well. It was found to be possible to package a prototypical Baeyer-Villiger monooxygenase, cyclohexanone monooxygenase (CHMO) [32]. Encapsulated CHMO did not show activity towards cyclohexanone, although CHMO has been packaged in a correctly folded state (FAD-bound) as suggested by the yellow appearance. In this case it is likely that NADPH, the coenzyme required for activity, is not able to enter the interior of the encapsulin. Pores of ~10 Å should allow passage of substrates of up to 800 g/mol [33]. Since the measured size of the pore is 9 Å and the molecular mass of NADPH is 744 g/mol it is likely that NADPH cannot pass through the pores. This observation may also provide an additional *raison d'être* for encapsulins: they function as molecular sieves for the enzymes that are in the encapsulins, thereby preventing undesired reactions. In contrast to CHMO, an encapsulated FAD-containing carbohydrate oxidase, mChitO [34], was found to be active when packaged in EncMh (Fig. S14). This oxidase accepts various oligosaccharides. All tested oligosaccharides (cellobiose, maltotriose and cellotetraose) were found to be oxidized, indicating that EncMh allows passage of such hydrophilic molecules, where the highest molar weight is the one of cellotetraose (667 g/mol), which fits within the expected molecular weight cut-off [33]. Furthermore, as was observed for the peroxidase, mChitO showed improved thermostability at 50 °C by retaining half of its initial activity after 4 h, while soluble, non-encapsulated mChitO loses most of its activity within 1 h (Fig. 4).

3.6. The use encapsulated peroxidase for the synthesis of lignin-like polymers

The compartmentalization of enzymes within encapsulin offers the possibility of tuning the substrate scope of the enzyme. The effect of added selectivity of enzymes encapsulated in EncMh was assessed by performing a cascade reaction involving SviDyP. Recently, we reported on the use of eugenol as starting material and eugenol oxidase and peroxidase as biocatalysts for the production of lignin-like material [35–37]. We tested the effect of using encapsulated SviDyP on the characteristics of the formed lignin oligomers. It was found that the packaged peroxidase can still support formation of lignin-like material as revealed by the formation of insoluble lignin-like oligomers. Interestingly, the end-product contains a slightly different relative abundance of the linkages as compared to the system where peroxidase is not

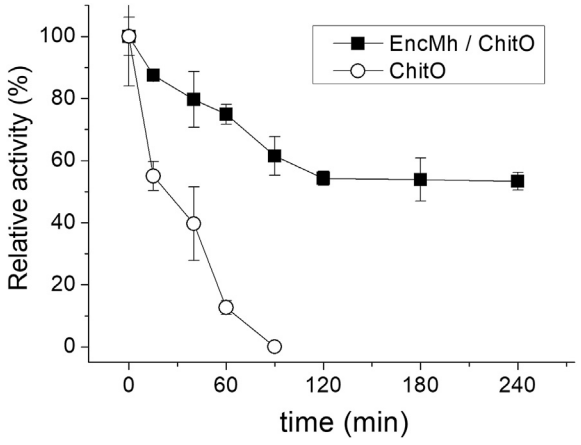

Fig. 4. The effect of encapsulation on stability of ChitO (X-axis for time of incubation at 50 °C; Y-axis, activity relative to the starting enzyme preparation).

encapsulated. This approach with encapsulated peroxidase resulted in a lower abundance of dibenzodioxin, b-O-4, b-b and b-5 linkages, while promoting formation of a-O-4 linkages (Table S1).

In summary, the results demonstrate that EncMh can be used to package all kinds of biocatalysts, including heme-, flavin- and metalloenzymes of different sizes and oligomerization states. Successful incorporation of cofactor containing enzymes shows that the enzymes are incorporated in the encapsulin nanocage after folding and cofactor incorporation. This is in line with the proposed mechanism of cargo loading which relies on association of the C-terminal cargo loading peptide to encapsulin protomers during the self-assembly process. This work also shows that the approach of coexpressing EncMh with a target protein provides a generic method for producing encapsulins loaded with any desired protein. While this concept has been shown in other studies, for example for creating artificial organelles in yeast [38] or size-selective RNA packaging and creation of artificial proteasomes [39,40], we now demonstrate that encapsulin-packaged enzymes can be used as biocatalysts. Through engineering of the encapsulin, it may also be possible to tune the catalytic properties of the enzyme. Recently, the groups of Lutz and Hilvert have shown that through modifying the pores of encapsulins or other protein-based cages, such cages attain specific permeation properties [34,39–41]. This concept of adding an additional filtering layer around an enzyme may also have been the evolutionary trigger for bacteria to evolve such protein-based nanocages.

Declaration of competing interest

The authors declare that they have no known competing financial interests or personal relationships that could have appeared to influence the work reported in this paper.

Acknowledgement

The authors are thankful to Dr. M. Trajković for help with interpretation of 2D NMR spectra of lignin oligomers and Dr. M.J.L.J. Fürst for help with creating the pENC vector.

Appendix A. Supplementary data

Supplementary data to this article can be found online at https://doi.org/10.1016/j.bbrc.2020.06.059.

References

[1] C.A. Kerfeld, C. Aussignargues, J. Zarzycki, F. Cai, M. Sutter, Bacterial microcompartments, Nat. Rev. Microbiol. 16 (2018) 277–290.
[2] T.W. Giessen, P.A. Silver, Widespread distribution of encapsulin nanocompartments reveals functional diversity, Nat. Mcrobiol. 2 (2017) 17029.
[3] I.J. Minten, V.I. Claessen, K. Blank, A.E. Rowan, R.J.M. Nolte, J.J.L.M. Cornelissen, Catalytic capsids: the art of confinement, Chem. Sci. 2 (2011) 358–362.
[4] M. Comellas-Aragones, H. Engelkamp, V.I. Claessen, N.A. Sommerdijk, A.E. Rowan, P.C. Christianen, J.C. Maan, B.J. Verduin, J.J. Cornelissen, R.J. Nolte, A virus-based single-enzyme nanoreactor, Nat. Nanotechnol. 2 (2007) 635–639.
[5] C. Cassidy-Amstutz, L. Oltrogge, C.C. Going, A. Lee, P. Teng, D. Quintanilla, A. East-Seletsky, E.R. Williams, D.F. Savage, Identification of a minimal peptide tag for in vivo and in vitro loading of encapsulin, Biochemistry 55 (2016) 3461–3468.
[6] C. Aussignargues, B.C. Paasch, R. Gonzalez-Esquer, O. Erbilgin, C.A. Kerfeld, Bacterial microcompartment assembly: the key role of encapsulation peptides, Commun. Integr. Biol. 8 (2015), e1039755.
[7] V.C. Kalel, R. Erdmann, Unraveling of the structure and function of peroxisomal protein import machineries, Subcell. Biochem. 89 (2018) 299–321.
[8] M. Sutter, D. Boehringer, S. Gutmann, S. Gunther, D. Prangishvili, M.J. Loessner, K.O. Stetter, E. Weber-Ban, N. Ban, Structural basis of enzyme encapsulation into a bacterial nanocompartment, Nat. Struct. Mol. Biol. 15 (2008) 939–947.
[9] T.W. Giessen, P.A. Silver, Converting a natural protein compartment into a nanofactory for the size-constrained synthesis of antimicrobial silver nanoparticles, ACS Synth. Biol. 5 (2016) 1497–1504.
[10] J. Snijder, M. van de Waterbeemd, E. Damoc, E. Denisov, D. Grinfeld, A. Bennett, M. Agbandje-McKenna, A. Makarov, A.J. Heck, Defining the stoichiometry and cargo load of viral and bacterial nanoparticles by Orbitrap mass spectrometry, J. Am. Chem. Soc. 136 (2014) 7295–7299.
[11] H. Moon, J. Lee, J. Min, S. Kang, Developing genetically engineered encapsulin protein cage nanoparticles as a targeted delivery nanoplatform, Biomacromolecules 15 (2014) 3794–3801.
[12] H. Moon, J. Lee, H. Kim, S. Heo, J. Min, S. Kang, Genetically engineering encapsulin protein cage nanoparticle as a SCC-7 cell targeting optical nanoprobe, Biomater. Res. 18 (2014) 21.
[13] I.J. Minten, R.J. Nolte, J.J. Cornelissen, Complex assembly behavior during the encapsulation of green fluorescent protein analogs in virus derived protein capsules, Macromol. Biosci. 10 (2010) 539–545.
[14] C.A. McHugh, J. Fontana, D. Nemecek, N. Cheng, A.A. Aksyuk, J.B. Heymann, D.C. Winkler, A.S. Lam, J.S. Wall, A.C. Steven, E. Hoiczyk, A virus capsid-like nanocompartment that stores iron and protects bacteria from oxidative stress, EMBO J. 33 (2014) 1896–1911.
[15] M. Kwak, I.J. Minten, D.M. Anaya, A.J. Musser, M. Brasch, R.J. Nolte, K. Mullen, J.J. Cornelissen, A. Herrmann, Virus-like particles templated by DNA micelles: a general method for loading virus nanocarriers, J. Am. Chem. Soc. 132 (2010) 7834–7835.
[16] R. Frey, T. Hayashi, D. Hilvert, Enzyme-mediated polymerization inside engineered protein cages, ChemComm 52 (2016) 10423–10426.
[17] T. Beck, S. Tetter, M. Kunzle, D. Hilvert, Construction of Matryoshka-type structures from supercharged protein nanocages, Angew. Chem. 54 (2015) 937–940.
[18] T.W. Giessen, P.A. Silver, A catalytic nanoreactor based on in vivo encapsulation of multiple enzymes in an engineered protein nanocompartment, Chembiochem 17 (2016) 1931–1935.
[19] P.C. Jordan, D.P. Patterson, K.N. Saboda, E.J. Edwards, H.M. Miettinen, G. Basu, M.C. Thielges, T. Douglas, Self-assembling biomolecular catalysts for hydrogen production, Nat. Chem. 8 (2016) 179–185.
[20] A. Tamura, Y. Fukutani, T. Takami, M. Fujii, Y. Nakaguchi, Y. Murakami, K. Noguchi, M. Yohda, M. Odaka, Packaging guest proteins into the encapsulin nanocompartment from *Rhodococcus erythropolis* N771, Biotechnol. Bioeng. 112 (2015) 13–20.
[21] W.L. DeLano, Pymol: an open-source molecular graphics tool, CCP4 Newslett. Protein Crystallogr. 40 (2002) 10.
[22] X. Robert, P. Gouet, Deciphering key features in protein structures with the new ENDscript server, Nucleic Acids Res. 42 (2014) W320–W324.
[23] I. Tiago, A. Maranha, V. Mendes, S. Alarico, P.J. Moynihan, A.J. Clarke, S. Macedo-Ribeiro, P.J. Pereira, N. Empadinhas, Genome sequence of *Mycobacterium hassiacum* DSM 44199, a rare source of heat-stable mycobacterial proteins, J. Bacteriol. 194 (2012) 7010–7011.
[24] M.M. Suhanovsky, C.M. Teschke, Nature's favorite building block: deciphering folding and capsid assembly of proteins with the HK97-fold, Virology (2015) 487–497.
[25] J.S. Plegaria, C.A. Kerfeld, Engineering nanoreactors using bacterial microcompartment architectures, Curr. Opin. Biotechnol. 51 (2018) 1–7.
[26] W. Yu, W. Liu, H. Huang, F. Zheng, X. Wang, Y. Wu, K. Li, X. Xie, Y. Jin, Application of a novel alkali-tolerant thermostable DyP-type peroxidase from *Saccharomonospora viridis* DSM 43017 in biobleaching of eucalyptus kraft pulp, PloS One 9 (2014), e110319.
[27] H. Contreras, M.S. Joens, L.M. McMath, V.P. Le, M.V. Tullius, J.M. Kimmey, N. Bionghi, M.A. Horwitz, J.A. Fitzpatrick, C.W. Goulding, Characterization of a *Mycobacterium tuberculosis* nanocompartment and its potential cargo proteins, J. Biol. Chem. 289 (2014) 18279–18289.
[28] M.W. Fraaije, J. Wu, D.P. Heuts, E.W. van Hellemond, J.H. Spelberg, D.B. Janssen, Discovery of a thermostable Baeyer-Villiger monooxygenase by genome mining, Appl. Microbiol. Biotechnol. 66 (2005) 393–400.
[29] E. van Bloois, D.E. Torres Pazmino, R.T. Winter, M.W. Fraaije, A robust and extracellular heme-containing peroxidase from *Thermobifida fusca* as prototype of a bacterial peroxidase superfamily, Appl. Microbiol. Biotechnol. 86 (2010) 1419–1430.
[30] N. Lončar, N. Božić, Z. Vujčić, Expression and characterization of a thermostable organic solvent-tolerant laccase from *Bacillus licheniformis* ATCC 9945a, J. Mol. Catal. B Enzym. 134 (2016) 390–395.
[31] N. Loncar, M.W. Fraaije, Not so monofunctional–a case of thermostable *Thermobifida fusca* catalase with peroxidase activity, Appl. Microbiol. Biotechnol. 99 (2015) 2225–2232.
[32] D.E. Torres Pazmino, H.M. Dudek, M.W. Fraaije, Baeyer-Villiger monooxygenases: recent advances and future challenges, Curr. Opin. Chem. Biol. 14 (2010) 138–144.
[33] E.M. Williams, S.M. Jung, J.L. Coffman, S. Lutz, Pore engineering for enhanced mass transport in encapsulin nanocompartments, ACS Synth. Biol. 7 (2018) 2514–2517.
[34] A.R. Ferrari, M. Lee, M.W. Fraaije, Expanding the substrate scope of chitooligosaccharide oxidase from *Fusarium graminearum* by structure-inspired mutagenesis, Biotechnol. Bioeng. 112 (2015) 1074–1080.
[35] D.I. Colpa, N. Loncar, M. Schmidt, M.W. Fraaije, Creating oxidase-peroxidase fusion enzymes as a toolbox for cascade reactions, Chembiochem 18 (2017) 2226–2230.
[36] M. Habib, M. Trajkovic, M.W. Fraaije, The biocatalytic synthesis of syringaresinol from 2,6-Dimethoxy-4-allylphenol in one-pot using a tailored oxidase/

peroxidase system, ACS Catal. 8 (2018) 5549–5552.
[37] M.H.M. Habib, P.J. Deuss, N. Lončar, M. Trajkovic, M.W. Fraaije, A biocatalytic one-pot approach for the preparation of lignin oligomers using an oxidase/peroxidase cascade enzyme system, Adv. Synth. Catal. 359 (2017) 3354–3361.
[38] Y.H. Lau, T.W. Giessen, W.J. Altenburg, P.A. Silver, Prokaryotic nanocompartments form synthetic organelles in a eukaryote, Nat. Commun. 9 (2018) 1311.
[39] Y. Azuma, D.L.V. Bader, D. Hilvert, Substrate sorting by a supercharged nanoreactor, J. Am. Chem. Soc. 140 (2018) 860–863.
[40] Y. Azuma, T.G.W. Edwardson, N. Terasaka, D. Hilvert, Modular protein cages for size-selective RNA packaging in vivo, J. Am. Chem. Soc. 140 (2) (2018) 566–569.
[41] Y. Azuma, M. Herger, D. Hilvert, Diversification of protein cage structure using circularly permuted subunits, J. Am. Chem. Soc. 140 (2018) 558–561.